Inorg. Chem. **2003**, *42*, 2288–2293

Photochemical Investigation of Roussin's Red Salt Esters: $Fe_2(\mu\text{-}SR)_2(NO)_4$

Christa L. Conrado, James L. Bourassa, Christian Egler, Stephen Wecksler, and Peter C. Ford*

Department of Chemistry and Biochemistry, University of California, Santa Barbara, California 93106-9510

Received May 2, 2002

The photochemistry of various Roussin's red ester compounds of the general formula $Fe_2(SR)_2(NO)_4$, where R = CH_3, CH_2CH_3, $CH_2C_6H_5$, CH_2CH_2OH, and $CH_2CH_2SO_3^-$, were investigated. Continuous photolyses of these ester compounds in aerated solutions led to the release of NO with moderate quantum yields for the photodecomposition of the ester (Φ_{RSE} = 0.02–0.13). Electrochemical studies using an NO electrode demonstrated that 4 mol of NO are generated for each mole of ester undergoing photodecomposition. Nanosecond flash photolysis studies of $Fe_2(SR)_2(NO)_4$ (where R = CH_2CH_2OH and $CH_2CH_2SO_3^-$) indicate that the initial photoreaction is the reversible dissociation of NO. In the absence of oxygen, the presumed intermediate, $Fe_2(SR)_2(NO)_3$, undergoes second-order reaction with NO to regenerate the parent cluster with a rate constant of $k_{NO} = 1.1 \times 10^9$ M^{-1} s^{-1} for R = CH_2CH_2OH. Under aerated conditions the intermediate reacts with oxygen to give permanent photochemistry.

Introduction

Nitric oxide (NO, also known as nitrogen monoxide) has been shown to sensitize cells to ionizing radiation;[2] thus, nitrosyl containing compounds are of interest as potential NO sources for physiological targets. One ongoing research theme of this laboratory has been the development of photochemical strategies to deliver nitric oxide to such targets on demand,[3,4] and we and others have probed a number of different compounds as potential photochemical precursors of NO.[3–5] Among these were the Roussin's "black salt" anion $Fe_4S_3(NO)_7^-$ (RBS) and "red salt" dianion $Fe_2S_2(NO)_4^{2-}$ (RRS). Both RBS and RRS are photoactive toward NO release;[3] however, cell culture experiments show RBS to be fairly toxic.[3a] The red salt is less toxic and more photoactive (Φ_{RRS} values ranging from 0.09 to 0.40 depending upon solvent and other conditions), and visible light photolysis of hypoxic V79 Chinese hamster cell cultures that had been treated with a submillimolar solution of RRS indicated marked sensitization of γ-radiation induced cell death. This effect was attributed to sensitization of radiation damage by NO released during the simultaneous photolysis.[3a] However, RRS is relatively unstable and, as a consequence, not likely to have practical application in more complex systems.

Related to RRS are a series of Roussin's "red esters" (RSEs), which can be prepared via the alkylation of the anion by reaction with an alkyl halide (eq 1).[6]

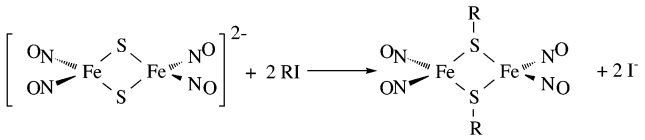

Preliminary experiments indicated that the esters were more stable than RRS while remaining photoactive toward NO release. Herein are described the results of photochemical studies of the following red ester compounds: the dimethyl

* To whom correspondence should be addressed. E-mail: ford@chem.ucsb.edu.

(1) Undergraduate student from Westfaelische Wilhelms-Universitaet, Muenster, Germany.

(2) (a) Howard-Flanders, P. *Nature (London)* **1957**, *180*, 1191. (b) Mitchell, J. B.; Wink, D. A.; DeGraff, W.; Gamson, J.; Keefer, L. K.; Krishna, M. C. *Cancer Res.* **1993**, *53*, 5845.

(3) (a) Bourassa, J.; DeGraff, W.; Kudo, S.; Wink, D. A.; Mitchell, J. B.; Ford, P. C. *J. Am. Chem. Soc.* **1997**, *119*, 2853−2860. (b) Kudo, S.; Bourassa, J. L.; Boggs, S. E.; Sato, Y.; Ford, P. C. *Anal. Biochem.* **1997**, *247*, 193−202. (c) Bourassa, J.; Lee, B.; Bernard, S.; Schoonover, J.; Ford, P. C. *Inorg. Chem.* **1999**, *38*, 2947−2952. (d) Bourassa, J. L.; Ford, P. C. *Coord. Chem. Rev.* **2000**, *200*−*202*, 887−900. (e) Bourassa, J. L. Ph.D. Dissertation, University of California, Santa Barbara, 1998.

(4) (a) Ford, P. C.; Bourassa, J.; Miranda, K.; Lee, B.; Lorkovic, I.; Boggs, S.; Kudo, S.; Laverman, L. *Coord. Chem. Rev.* **1998**, *171*, 185−202. (b) Lorkovic, I. M.; Miranda, K. M.; Lee, B.; Bernhard, S.; Schoonover, J. R.; Ford, P. C. *J. Am. Chem. Soc.* **1998**, *120*, 11674−11683. (c) De Leo, M.; Ford P. C. *J. Am. Chem. Soc.* **1999**, *121*, 1980−1981. (d) Works, C. F.; Ford, P. C. *J. Am. Chem. Soc.* **2000**, *122*, 7592−7593.

10.1021/ic020309e CCC: $25.00 © 2003 American Chemical Society
Published on Web 03/06/2003

ester, $Fe_2(\mu\text{-}SCH_3)_2(NO)_4$ (**1**), the diethyl ester, $Fe_2(\mu\text{-}SCH_2CH_3)_2(NO)_4$ (**2**), the dibenzyl ester $Fe_2(\mu\text{-}CH_2C_6H_5)_2(NO)_4$ (**3**), the 2-hydroxyethyl ester, $Fe_2(SCH_2CH_2OH)_2(NO)_4$ (**4**), and the 2-sulfonato-ethyl ester, $Na_2[Fe_2(SCH_2CH_2SO_3)_2(NO)_4]$ (**5**).

Experimental Section

Materials. Water for spectroscopic studies was purified by a Millipore system. Methanol was distilled under nitrogen from I_2 and Mg. Acetonitrile was distilled under dinitrogen from CaH_2 and used immediately. Chromatographic grade argon was purchased from Air Liquide and used as received. All inert atmosphere manipulations were performed on a vacuum manifold. Deaeration of the solutions was achieved by 3 freeze−pump−thaw (f-p-t) cycles. Nitric oxide (99.0%) was purchased from Matheson and passed through a stainless steel column that contained Ascarite II (NaOH on a silicate carrier) to remove higher nitrogen oxides. Stainless steel tubing and fittings were used to transfer gases. Manifold connections were accomplished by using stainless steel-to-glass fittings.

Instruments. UV−vis absorption spectra were recorded for solutions in 1 cm path length quartz cells using a HP8572 diode array spectrophotometer. Infrared spectra were obtained using a BioRad FTS 60 SPC 3200 FTIR spectrometer and IR cells equipped with CaF_2 windows.

Photochemical Experiments. Solutions for continuous photolysis experiments were generally about 10^{-4} M in RSE concentration while those for flash experiments were in the range 35−40 mM. All continuous and flash experiments were carried out at 295 (±1) K. Quartz photolysis cells (1.0 cm) were used in both types of experiments. When a controlled atmosphere (Ar, NO, or O_2) was necessary, the photolysis cell consisted of a triple O-ring Chemglass Teflon stopcock, a four-sided quartz cuvette, and an O-ring adapter for connection to a gas/vacuum manifold. Concentrations were calculated from published solubility data.[7]

Continuous photolyses (CW) were performed using an optical train with an Oriel 200 W Hg arc lamp in an Oriel lamp housing model 66033 as the light source. Interference filters were used to isolate the appropriate excitation wavelengths. Chemical actinometry was performed with ferric oxalate solutions.[8] All solutions in the CW experiments were stirred continuously and kept from exposure to extraneous light.

The quantitative determination for the photochemical production of Fe^{2+} from the ester complexes was accomplished by adding a 1,10-phenanthroline solution and recording the intensity of the characteristic 510 nm absorbance of the $Fe(phen)_3^{2+}$ species formed. Addition of 1,10-phen to RSE solutions which had not been photolyzed did not lead to significant 510 nm absorbance changes over the time frame of the analytical procedure.

Flash photolysis experiments were carried out on a time-resolved optical (TRO) apparatus described previously.[4b] The pump source was a Continuum NY60-20 nanosecond pulse Nd:YAG laser operating in the third harmonic (355 nm) and attenuated to 10−30 mJ/pulse. The probe source was a high pressure, short arc xenon lamp. Kinetic traces were obtained using a SPEX Doublemate monochromator and RCA model 8852 PMT for detection. The eventual photolysis product is an orange solid that would build up on the laser cell after repetitive laser flashes, and formation of such solids could potentially compromise the data collection for a given experiment. For this reason, fresh 3 mL aliquots of the ester solutions were flashed a maximum of 10 times each, and the solutions were shaken between each flash experiment. Such procedures reduced the opportunity for improving signal/noise ratio by signal averaging.

Syntheses. The Roussin's red ester compounds were prepared by literature methods.[6b] These esters are moderately air and light sensitive and require long-term storage in the dark and under inert atmosphere.

$Fe_2(\mu\text{-}SCH_3)_2(NO)_4$ (1), $Fe_2(\mu\text{-}CH_2CH_3)_2(NO)_4$ (2), $Fe_2(\mu\text{-}CH_2C_6H_5)_2(NO)_4$ (3), and $Fe_2(\mu\text{-}SCH_2CH_2OH)_2(NO)_4$ (4).[6] The methyl ester **(1)** was prepared by the procedure described by Seyferth and co-workers.[6b] Similar procedures were followed to prepare $Fe_2(\mu\text{-}SCH_2CH_3)_2(NO)_4$ **(2)** and $Fe_2(\mu\text{-}SCH_2C_6H_5)_2(NO)_4$ **(3)** with the exception that iodoethane, benzyl iodide, or 2-iodoethanol was used, respectively, instead of iodomethane. These compounds were characterized by both IR and UV−vis spectroscopy. (**1**). UV−vis (MeOH) (λ_{max} in nm (ϵ in M^{-1} cm^{-1})): 312 (8.3×10^3), 364 (7.8×10^3). IR (CH_3CN) (ν_{max} in cm^{-1} (ϵ in M^{-1} cm^{-1})): 1778 (5.8×10^3), 1752 (5.3×10^3), 1800 (w). (**2**). UV−vis (CH_3CN): 310 (9.1×10^3), 364 (8.7×10^3). IR (CH_3CN): 1776 (5.9×10^3), 1750 (5.2×10^3), 1800 (w). (**3**). UV−vis ($CHCl_3$): 312 (9.3×10^3), 364 (8.5×10^3). IR ($CHCl_3$): 1778 (5.5×10^3), 1751 (5.0×10^3), 1800 (w). FAB (NBA matrix): *m*/*z* 448 $(Fe_2(SCH_2C_6H_5)_2(NO)_3)^+$, 418 $(Fe_2(\mu\text{-}SCH_2C_6H_5)_2(NO)_2^+$. (**4**). UV−vis (MeOH): 312 (9.3×10^3), 362 (8.5×10^3). IR (MeOH): 1778 (5.8×10^3), 1752 (5.6×10^3), 1800 cm^{-1} (w). ESI (methanol/water): *m*/*z* 386 $(Fe_2(SCH_2CH_2OH)_2(NO)_4]^-)$.

$Na_2[Fe_2(\mu\text{-}SCH_2CH_2SO_3)_2(NO)_4]$ (5). A solution of $Na_2[Fe_2S_2(NO)_4]\cdot 8H_2O$ (RRS) (1.0 g; 2.1 mmol) plus the sodium salt of bromoethanesulfonic acid (1.0 g; 4.7 mmol) in 75 mL of deoxygenated water was prepared. The mixture was stirred under argon, and then the solution was heated at reflux under argon for 1 h. The volume was reduced by rotary evaporation to approximately 10 mL and was then cooled to 5 °C. The result was a crop of shiny, brownish-red crystals. The product was recrystallized from a minimum volume of hot water and stored under argon in a refrigerator. The product was characterized by UV−vis and IR spectroscopy and ESI MS. The UV−vis spectrum was similar to those seen for the other ester compounds.[6] UV−vis (H_2O) (λ_{max} in nm (ϵ in M^{-1} cm^{-1})): 310 (9.2×10^3), 364 (8.9×10^3). IR (CH_3CN) (ν_{max} in cm^{-1} (ϵ in M^{-1} cm^{-1})): 1782 (5.6×10^3), 1757 (5.8×10^3), 1821 (w). Aqueous solution negative ion ESI-MS *m*/*z* (relative intensity): 535 (18) $[(Fe_2(SCH_2CH_2SO_3)_2(NO)_4)Na]^{1-}$, 505 (21) $[(Fe_2(SCH_2CH_2SO_3)_2(NO)_3)Na]^{1-}$, 483 (12) $[(Fe_2(SCH_2CH_2SO_3)_2(NO)_3),H]^{1-}$, 372 (5) $[(Fe_2(SCH_2CH_2SO_3)(NO)_4)]^{1-}$, 342 (8) $(Fe_2(SCH_2{-}CH_2SO_3)_1(NO)_3]^{1-})$, 256 (48)$([Fe(SCH_2CH_2SO_3)(NO)_2]^{1-})$, 226 (100) $([Fe_1(SCH_2{-}CH_2SO_3)_1(NO)_1]^{1-})$. CHN elemental analysis Calcd for $C_4H_8N_4O_{10}S_4Fe_2Na_2\cdot(3\ H_2O)$: C, 7.84; H, 2.29; N, 9.15. Found (UCSB Marine Biology Analytical Labs): C, 7.87; H, 2.05; N, 8.67. Iron analysis by flame atomic

(5) (a) Flitney, F. W.; Megson, I. L.; Thomson, J. L. M.; Kennovin, G. D.; Butler, A. R. *Br. J. Pharmacol.* **1996**, *117*, 1549. (b) Carter, T.; Bettache, N.; Corrie, J. E. T.; Ogden, D.; Trentham, D. R. *Methods Enzymol*. **1996**, *268*, 266−281. (c) Namiki, S.; Kaneda, F.; Ikegami, M.; Arai, T.; Fujimori, K.; Asada, S.; Hama, H.; Kasuyua, Y.; Goto, K. *Bioorg. Med. Chem*. **1999**, *7*, 1695−1702. (d) Fukuhar, K.; Kurihara, M.; Miyata, N. *J. Am. Chem. Soc.* **2001**, *123*, 8662−8666.

(6) (a) Glidewell, C.; Lambert, R. J.; Harman, M. E.; Hursthouse, M. B. *J. Chem. Soc., Dalton Trans*. **1990**, 2685−2690. (b) Seyferth, D.; Gallagher, M. K.; Cowie, M. *Organometallics* **1986**, *5*, 539−548. (c) Sung, S. S.; Glidewell, C.; Butler, A. R.; Hoffman, R. *Inorg. Chem*. **1985**, *24*, 3856. (d) Butler, A. R.; Glidewell, C.; Hyde, A. R.; McGinnis, J. *Inorg. Chem*. **1985**, *24*, 2931−2934. (e) Thomas, J. T.; Robertson, J. H.; Cox, E. G. *Acta Crystallogr*. **1958**, *11*, 599.

(7) Battino, R.; Clever, H. L.; Young, C. L. *IUPAC Solubility Data Series*; Pergamon Press: New York, 1985; Vol. 8, p 261.

(8) Calvert, J. G.; Pitts, J. N. *Photochemistry*; Wiley: New York, 1967; pp 783−786.

absorption (Varian Techtron AA6 spectrophotometer) Calcd: Fe, 18.3. Found: Fe, 19.1 (± 1.0). An X-ray crystal structure has been obtained for the Ph_4As^+ salt of the $Fe_2(\mu\text{-}SCH_2CH_2SO_3)_2(NO)_4^{2-}$ anion with an *R*-factor about 6.3% confirming that this species has a structure consistent with the other esters as illustrated qualitatively in eq 1.[9]

Results

Spectroscopic Properties of RSE Compounds. The infrared NO stretching bands ν_{NO} of the RSE compounds $Fe_2(\mu\text{-}SR)_2(NO)_4$ are largely insensitive to the nature of the R group[5,6] but are markedly shifted to higher frequency compared to the bands seen for $Na_2[RRS]$ (~1665 cm^{-1}, 1690 cm^{-1}). For example, the FTIR spectra of $Fe_2(\mu\text{-}SCH_3)_2(NO)_4$ (**1**), $Fe_2(\mu\text{-}SCH_2CH_3)_2(NO)_4$ (**2**), $Fe_2(\mu\text{-}CH_2C_6H_5)_2(NO)_4$ (**3**), and $Fe_2(SCH_2CH_2OH)_2(NO)_4$ (**4**) each display two strong nitrosyl stretching bands of similar intensity at ~1750−1754 cm^{-1} ($\epsilon \sim 5.0-5.6 \times 10^3$ M^{-1} cm^{-1}) and ~1776−1778 cm^{-1} (~$5.5-5.9 \times 10^3$ M^{-1} cm^{-1}) as well as a weak band at 1800 cm^{-1} (200 M^{-1} cm^{-1}).[6] The nitrosyl stretches of the sulfonated species, $Na_2[Fe_2(SCH_2CH_2SO_3)_2(NO)_4]$ (**5**), are shifted slightly to 1757, 1782, and 1815 cm^{-1} in acetonitrile. The ν_{NO} bands show typical broadening in polar solvents; for instance, the bandwidths at half-maximum intensity for $Fe_2(\mu\text{-}SCH_3)_2(NO)_4$ range from 4 cm^{-1} in cyclohexane to 12 cm^{-1} in acetonitrile, but the band strengths and positions are not affected significantly by changing solvent. Notably, the much lower ν_{NO} band frequencies for the red salt anion $[Fe_2(\mu\text{-}S)_2(NO)_4]^{2-}$ are consistent with the greater back-donation of electron density from the dianionic $Fe_2(\mu\text{-}S)_2$ core into NO π^* orbitals.

The electronic spectra of the esters are also essentially independent of the R-group in the near-UV−vis region. Solutions of **1**, **2**, **3**, and **4** each show absorption bands with λ_{max} at ~312 nm (~9×10^3 M^{-1} cm^{-1}) and ~362 nm (~8.5×10^3 M^{-1} cm^{-1}) with a shoulder at ~430 nm (~4×10^3 M^{-1} cm^{-1}) that tails out into the green (~5×10^2 M^{-1} cm^{-1} at 550 nm). These spectra are analogous to the spectrum of aqueous RRS, which shows bands at 314 nm (8.5×10^3 M^{-1} cm^{-1}) and 374 nm (10.4×10^3 M^{-1} cm^{-1}) as well as a stronger band at 242 nm (2.8×10^4 M^{-1} cm^{-1}). For the Roussin's salts, EHMO calculations suggested that the LUMO for the iron−sulfur cluster has Fe−NO antibonding character consistent with the photolability seen.[6c] We assume that the electronic transitions for these RSE compounds are similar to those seen for RRS.

Photoreactions of Roussin's Red Esters: CW Photolyses. In the dark, the RSE compounds are thermally stable over a period of 30 h in deoxygenated solutions and show only ~10% thermal decomposition over 3 h in aerated solutions. As noted already, the extinction coefficients for all the ester compounds are nearly 10^4 M^{-1} cm^{-1} for each λ_{max}. However, these compounds were reactive under continuous photolysis with near-UV or visible light when dissolved in aerated solvents. This is illustrated by Figure 1, which shows the typical spectral changes across the near-UV−vis spectrum when one of the esters, in this case methanolic $Fe_2(SCH_2CH_2OH)_2(NO)_4$, is irradiated in aerated solution. The quantum yields for RSE photodecomposition (Φ_d) were determined from the quantitative UV−Vis absorption changes upon photolysis for solutions equilibrated with oxygen or with air and with RSE concentrations of 76−100 μM. These are summarized in Table 1 for various esters studied under a variety of conditions. In general, the IR spectra of photolyzed RSE solutions under aerated conditions showed the loss of the parent ν_{NO} bands, and no new bands in the NO stretching frequency region appeared suggesting the absence of a long-lived metal−nitrosyl intermediate or product. (Free NO has a low extinction coefficient and would not have been detected under these conditions.)

The Φ_d values for the various RSEs under continuous

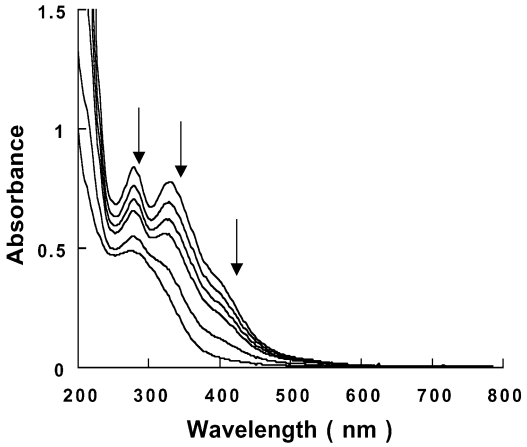

Figure 1. Spectral changes recorded during the continuous photolysis (λ_{irr} = 365 nm) of $Fe_2(SCH_2CH_2OH)_2(NO)_4$ (85 μM, initial concentration) in aerated methanol ([O_2] = 1.8 mM, T = 294 K). The second, third, and fourth spectra were recorded after successive 2 min photolysis intervals.

Table 1. Quantum Yields for Ester Photodecomposition under Various Conditions[a]

medium	λ_{irr} (nm)	I_a (Ein/L s)	Φ_d (mol/Ein)
	$Fe_2(\mu\text{-}SCH_3)_2(NO)_4$ (**1**)		
MeOH	365	3.0×10^{-6}	0.14 ± 0.02
CH_3CN	365	3.0×10^{-6}	0.23 ± 0.05
CH_2Cl_2	365	3.0×10^{-6}	0.07± 0.03
THF	365	3.0×10^{-6}	0.28 ± 0.02
	$Fe_2(\mu\text{-}SCH_2CH_3)_2(NO)_4$ (**2**)		
CH_3CN	365	1.1×10^{-6}	0.076 ± 0.004
CH_3CN[b]	365	1.1×10^{-6}	0.12 ± 0.01
CH_3CN[c]	365	1.1×10^{-6}	<0.003
$CHCl_3$	546	1.1×10^{-6}	$(1.7 \pm 0.2) \times 10^{-4}$
	$Fe_2(\mu\text{-}SCH_2C_6H_5)_2(NO)_4$ (**3**)		
$CHCl_3$	436	1.1×10^{-6}	$(3.2 \pm 0.1) \times 10^{-4}$
$CHCl_3$	546	1.1×10^{-6}	$(1.9 \pm 0.2) \times 10^{-4}$
	$Fe_2(\mu\text{-}SCH_2CH_2OH)_2(NO)_4$ (**4**)		
MeOH	365	1.1×10^{-6}	0.079 ± 0.005
MeOH	365	3.0×10^{-6}	0.045 ± 0.003
MeOH	365	8.2×10^{-6}	0.020 ± 0.003
MeOH[b]	365	1.1×10^{-6}	0.103 ± 0.009
MeOH	405	6.0×10^{-7}	0.132 ± 0.01
MeOH	405	1.7×10^{-6}	0.056 ± 0.003
MeOH	405	1.0×10^{-6}	0.052 ± 0.003
	$Na_2[Fe_2(\mu\text{-}SCH_2CH_2SO_3)_2(NO)_4]$ (**5**)		
H_2O	365	1.1×10^{-6}	0.024 ± 0.001
H_2O[c]	365	1.1×10^{-6}	0.052 ± 0.005
H_2O	365	3.0×10^{-6}	0.048 ± 0.004

[a] Quantum yields for RSE decomposition determined from changes in UV−vis spectra. Experiments in aerated solutions at 294 K, except where noted. Values reported are from 3 or more independent determinations. Initial RSE concentrations for these continuous photolysis experiments were ~10^{-4} M. [b] Solutions equilibrated with O_2 (1 atm). [c] Deaerated solution.

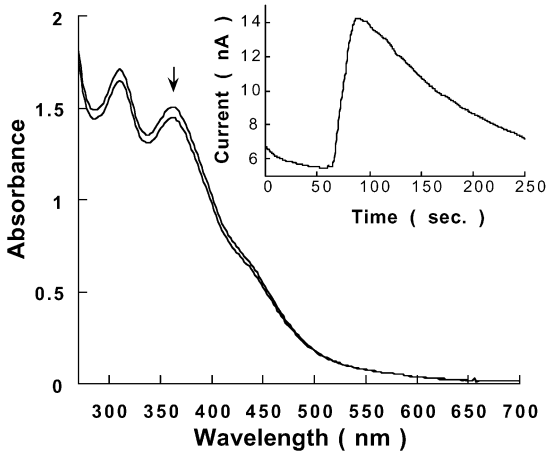

Figure 2. Quantitative determination of NO production upon irradiation of Roussin's salt ester $Na_2[Fe_2(\mu SCH_2CH_2SO_3)_2(NO)_4]$. UV−vis absorbance changes and NO sensor amperogram upon white light photolysis of an aerated pH 7 phosphate buffered solution at 294 K. $\Delta[NO]/\Delta[ester] = 3.7$.

photolysis proved to be systematically dependent upon several key factors (Table 1) including excitation wavelength, λ_{irr}, and intensity, I_a. For example, Φ_d tended to fall off at longer excitation wavelength λ_{irr} and at higher I_a. Another factor was the oxygen concentration in the solution. For example, there is little net photodecomposition ($\Phi_d < 0.003$) in deaerated acetonitrile solutions of **2** with $I_a = 6.1 \times 10^{-6}$ Ein/L·s at 365 nm, but Φ_d rose to 0.076 in aerated solution and to 0.12 in solution equilibrated with O_2 at 1 atm under otherwise analogous conditions. This behavior parallels the quantitative photochemistry of Roussin's red and black salts[3] and can be attributed to the primary photoreaction step being the reversible labilization of one NO to give transient species that must be trapped by O_2 in order to give permanent photoreaction (see later). The oxygen dependence also explains the quantum yield results in different solvents. One can see from Table 1 that solvents in which O_2 is more soluble reveal the larger Φ_d values in air equilibrated systems.

Products from the CW Photolysis of 5. Continuous photolysis of aqueous $Na_2[Fe_2(\mu\text{-}SCH_2CH_2SO_3)_2(NO)_4]$ demonstrated that the ester complexes release 4 NOs for every molecule of ester decomposed (Figure 2). The quantitative analyses were carried out for aerated aqueous phosphate buffer solutions (pH = 7) using the combination electrode NO sensor. The Pyrex and IR filtered output of a mercury arc lamp with a 365 nm interference filter was used for the photolysis. The change in [**5**] upon photolysis was evaluated by changes in the solution absorption spectra, and the [NO] produced was evaluated from the amperogram. These procedures gave the reaction stoichiometry ratio $\Delta[NO]/\Delta[RSE] = 4.1 \pm 0.2$ for **5** in aqueous solution. In the absence of other NO sinks, it is presumed that aqueous autoxidation leads primarily to nitrite as the eventual product. A similar study with $Fe_2(\mu\text{-}SCH_2CH_2OH)_2(NO)_4$ in 5% aq methanol gave the ratio 3.8 ± 0.3.

Other products of CW photolysis of aqueous $Na_2[Fe_2(\mu\text{-}SCH_2CH_2SO_3)_2(NO)_4]$ include NO_2^-, free ligand $HSCH_2CH_2SO_3^-$, and minor amounts of NO_3^- as seen by electrospray ionization mass spectral (ESI-MS) analysis. Additionally, the formation of Fe^{2+} was verified by the addition of 1,10-phenanthroline (phen) to give $Fe(phen)_3^{2+}$ with a characteristic strong absorbance at 510 nm. Aerated aqueous solutions of **5** (~70 mM) were monitored spectrophotometrically during 365 nm photolysis until the RSE photodecomposition was approximately 20%. Then, a 1.0 mL aliquot of this solution was diluted with a 1.0 mL volume of water, and the UV−vis absorption spectrum was taken (for a baseline). Another 1.0 mL aliquot was added to a 1.0 mL volume of phen solution (5.5 mM), and the spectrum was recorded after allowing the solutions to develop. The result was the characteristic, strong absorptions at the λ_{max} (510 nm, $\epsilon_{510} = 1.11 \times 10^4\ M^{-1}\ cm^{-1}$) of $Fe(phen)_3^{2+}$. RSE solutions that had not been irradiated gave negligible positive tests for Fe(II) formation after correcting for the baseline solution spectrum. The absorbance changes in the photolysis solution of **5** indicated the amount of RSE decomposed, while the phenanthroline analyses determined the concentration of Fe^{2+} generated and from these a product yield ratio of 2.4 ± 0.3 mol of Fe(II) generated per mole of **5** photodecomposed was calculated. The final photoproduct solution is thus presumed to include various ferrous−thiol complexes. Consistent with this view was the observation that the product spectrum can be duplicated by mixing ferrous solutions with mercaptoethanol and nitrite.

Flash Photolysis Experiments. Flash photolysis studies were carried out for solutions of $Fe_2(\mu\text{-}SCH_3)_2(NO)_4$ (**1**) in acetonitrile, $Fe_2(\mu\text{-}SCH_2CH_2OH)_2(NO)_4$ (**4**) in methanol, and $Na_2[Fe_2(\mu\text{-}SCH_2CH_2SO_3)_2(NO)_4]$ (**5**) in water. The behavior for all three systems was qualitatively similar. Namely, 355 nm flash photolysis led to bleaching of the visible range absorbance monitored at 450 nm, which decayed quickly back to the baseline absorbance when excess NO was present, and much more slowly under an inert atmosphere. The latter observation is consistent with the result of the continuous photolysis experiments that indicated virtually no net photoreaction in the absence of oxygen. In this context, when the flash photolysis was carried out using aerated solutions, only partial recovery of the initial absorbance at 450 nm was observed, again consistent with the continuous photolysis experiments that demonstrated oxygen to be required for net photoreaction.

An example of the behavior in deaerated solution would be the 355 nm flash photolysis of methanolic $Fe_2(\mu\text{-}SCH_2CH_2OH)_2(NO)_4$ under argon. Transient bleaching of the absorbance at 450 nm was seen, and this decayed back to baseline over the course of several hundred microseconds. The decay did not fit well to an exponential function but could be fit adequately according to second-order kinetics (1/abs versus t is linear) as expected if the primary photoreaction is reversible NO labilization to give the reactive intermediate $Fe_2(\mu\text{-}SR)(NO)_3$ ($\mathbf{I_1}$) and this is followed by second-order recombination of $\mathbf{I_1}$ and NO (eq 2).

$$Fe_2(\mu\text{-}SR)_2(NO)_4 \underset{k_{NO}}{\overset{h\nu}{\rightleftharpoons}} \underset{\mathbf{I_1}}{Fe_2(\mu\text{-}SR)_2(NO)_3} + NO \qquad (2)$$

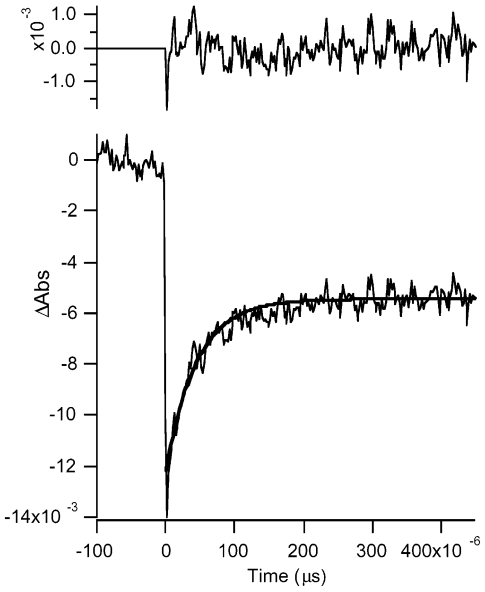

Figure 3. Flash photolysis of $Fe_2(\mu\text{-}SCH_2CH_2OH)_2(NO)_4$ (36.3 μM) in aerated methanol as monitored at 420 nm ($[O_2] = 1.8$ mM; $T = 294$ K). The solid line is the exponential fit for the temporal absorbance change. The residual to that fit is illustrated at the top of the figure.

The 355 nm flash photolysis of **4** in *aerated* methanol showed analogous initial transient bleaching at 420 nm but with much faster absorbance changes. While the absorbance due to the ester recovers partially, it does not return to the initial value within the monitoring time (500 μs). The decay of this transient bleach fits a simple exponential with $k_{obs} = 2.3 \times 10^4$ s^{-1} (295 K) (Figure 3). If one assumes that this decay is largely the result of O_2 trapping of $\mathbf{I_1}$, an estimate of $k_{O2} = 1.3 \times 10^7$ M^{-1} s^{-1} can be made for the rate constant for this reaction (see later). For comparison, a k_{O2} value of 5.6×10^7 M^{-1} s^{-1} was determined previously for the O_2 trapping of analogous intermediates formed in the aqueous solution flash photolysis of RRS.[3]

Figure 4 illustrates the situation when the flash experiment was carried out under added NO. The example shown in this case is the 355 nm flash photolysis of aqueous $Na_2[Fe_2(\mu\text{-}SCH_2CH_2SO_3)_2(NO)_4]$ (**5**) equilibrated with a NO partial pressure P_{NO} of 613 Torr ([NO] = 1.07 mM). Again, immediate transient bleaching was observed (as monitored in this case at 420 nm), followed by decay back to the initial absorbance to regenerate the parent. However, in contrast to Figure 3, the reaction is completed within a few microseconds. The temporal absorbance follows exponential kinetics, and the fit shown in Figure 4 gives a k_{obs} of 1.7×10^6 s^{-1} ($T = 295$ K). When analogous experiments were carried out with aqueous **5** at different P_{NO} values, the k_{obs} values obtained were markedly dependent on [NO]. A plot of k_{obs} versus [NO] for five values of [NO] ranging from 0.1 to 2 mM proved to be linear, consistent with the relationship $k_{obs} = k_{NO}[NO]$ that is predicted by eq 2. The slope of this line gave $k_{NO} = (1.1 \pm 0.1) \times 10^9$ M^{-1} s^{-1} ($R^2 = 0.998$), only about an order of magnitude smaller than the diffusion limit under these conditions.

The flash data recorded under *aerated* conditions demonstrated that, in contrast to the situation under a NO or argon, permanent photochemistry occurs in the presence of

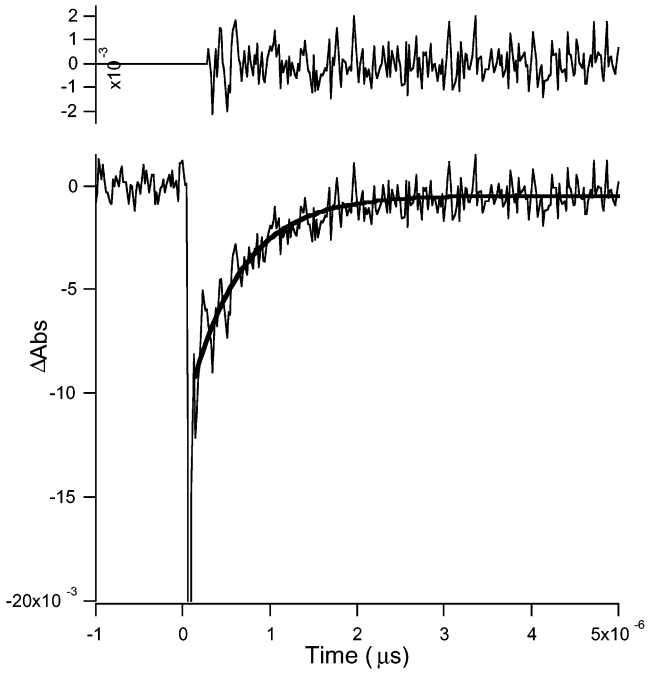

Figure 4. Flash photolysis of $Na_2[Fe_2(\mu\text{-}SCH_2CH_2SO_3)_2(NO)_4]$ (36.3 μM) in aqueous solution under NO (1.07 mM) as monitored at 420 nm. The solid line is the exponential fit for the temporal absorbance change. The residual to that fit is illustrated at the top of the figure.

Scheme 1

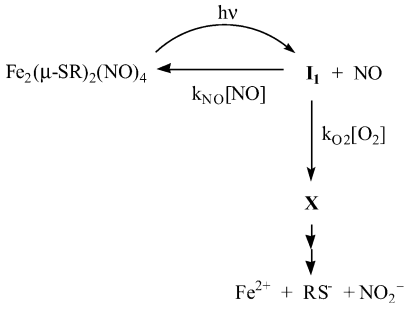

O_2. The flash data can be interpreted according to Scheme 1, which indicates the competition between NO and O_2 for the intermediate $\mathbf{I_1}$. It is assumed in this model that O_2 traps this intermediate to give one or more new species X that decompose irreversibly to the final products. NO is also known to react with O_2 via third-order kinetics to give (in aqueous solution) the nitrite ion.[10] However, while NO autoxidation is the likely fate of the NO generated in an aerobic environment, this process must be orders of magnitude slower than the O_2 trapping of $\mathbf{I_1}$ inferred by the continuous and flash photolysis experiments described here. Given that k_{NO} is about 10^9 M^{-1} s^{-1}, the fast reaction of $\mathbf{I_1}$ with the generated NO competes with trapping of the intermediate $\mathbf{I_1}$ by the dissolved O_2 ($k \sim 1.1 \times 10^7$ M^{-1} s^{-1}).

According to the scheme, the overall quantum yield for RSE photodecomposition will depend on the quantum yield for the primary NO labilization (ϕ_1), the concentration of O_2 present, and the steady state concentration of NO formed

(9) Wecksler, S.; Bu, X.; Ford, P. C. To be published
(10) Ford, P. C.; Wink, D. A.; Stanbury, D. M. *FEBS Lett.* **1993**, *326*, 1−3.

under continuous photolysis ($[NO]_{ss}$) as indicated by eq 3: If the intensity of absorbed light (I_a) is constant, then increasing $[O_2]$ increases Φ_d as was observed (Table 1). However, the steady state concentrations of $\mathbf{I_1}$ and of NO ($[NO]_{ss}$)[11] are both dependent on I_a, so at higher intensity, the competitive back reaction between these is enhanced relative to the pseudo-first-order trapping by oxygen. Qualitatively, at constant $[O_2]$ (e.g., an aerated solution), Φ_d should decrease with increasing intensity, and this was indeed observed (Table 1). In the limiting condition of very low I_a, the $k_{O_2}[O_2]$ term would be much greater than $k_{NO}[NO]$, and $\Phi_d \sim \phi_1$. A more quantitative test of this model was previously carried out with aqueous solutions of RRS.[3a]

In summary, Roussin's red salt esters have the potential to be efficient photochemical NO generators, and the pattern of photochemical behavior appears qualitatively the same among the various RSEs described here. Quantum yields for RSE decomposition range from ~0.02 to 0.13, depending on the ester, the intensity of light absorbed, and the solvent medium. Production of 4 mol of NO for each 1 mol of ester undergoing photoconversion was demonstrated by an electrochemical NO sensor. Flash photolysis experiments indicated that the primary photoreaction is the labilization of a single NO to give intermediate $\mathbf{I_1}$, presumably $Fe_2(\mu\text{-}SR)_2(NO)_3$, which is trapped by oxygen in competition with the very fast second-order back reaction to generate the initial RSE. Ongoing studies in this laboratory are concerned with the preparation and photochemical properties of new esters tailored to have pendent R-groups with defined biological or photooptical properties. For example, such pendant groups may act as an antenna to increase the efficiency of longer wavelength irradiation for the photochemical generation of NO or display some aspect of biological specificity.

$$\Phi_d = \frac{\frac{-d[RSE]}{dt}}{I_a} = \left[\frac{k_{ox}[O_2]}{k_{ox}[O_2] + k_{NO}[NO]_{ss}}\right]\phi_1 \qquad (3)$$

Acknowledgment. These studies were supported by the National Science Foundation (Grants CHE 9726889 and CHE 0095144). We thank Dr. X. Bu of this department for confirming the identity of the anion of compound **5** by determining the X-ray crystal structure.

IC020309E

(11) A referee has correctly noted that, in the absence of another sink for NO, the trapping of $\mathbf{I_1}$ by O_2 would lead to a build up of [NO], rather than a steady state concentration, $[NO]_{ss}$. However, the electrochemical measurement shown in Figure 2 illustrates that other processes, mostly autoxidation[9] in competition with diffusion out of the solution, deplete NO on a time scale (minutes) comparable to the continuous photolysis experiment, so [NO] has the potential to achieve a steady state dependent on the intensity of absorbed light, I_a. Although the function describing the temporal concentration of NO must be complex owing to the competing processes, the qualitative behavior of Φ_d in response to changes in I_a or $[O_2]$ is consistent with the description offered by eq 3.